2018 IEEE-RAS 18th International Conference on Humanoid Robots (Humanoids)
Beijing, China, November 6-9, 2018

Cylindrical Inverted Pendulum Model for Three Dimensional Bipedal Walking

Runming Zhang[1], Huaxin Liu[12], Fei Meng[12], Aiguo Ming[123], and Qiang Huang[12]

Abstract— **Energy efficiency of biped walking is an crucial topic for humanoid robot's research. Rapid computing is also important for online planning and model transplantation. Many dynamic models for characterizing humanoids' walking have been developed, such as conventional 3 dimensional inverted pendulum (IPM), linear inverted pendulum (LIPM). This paper proposed an improved inverted pendulum model constrained on cylindrical surface (CIPM), combining the advantages of computing and energy efficiency for humanoids' walking planning. Walking patterns with different speeds can be generated by CIPM. The constraint of cylindrical surface results in low coupling between displacement variables for tested robot and the energy consumption is less than that generated based on LIPM. The advantages of CIPM over IPM and LIPM were proved by mathematic analysis, simulations of bipedal walking with different speeds.**

I. Introduction

In previous humanoid robot investigations, the theory of multi-rigid-bodies dynamics, feedback controlling and motion stabilizing have been mostly applied. The inverted pendulum model (IPM) is a fundamental theory for bipedal walking research [1] [2]. Varieties of bipedal walking control models in base of IPM have been developed. Kajita proposed the theory of linear inverted pendulum (LIPM) [3]. This model restricts the height of the center of mass (COM) of the robot during walking, an then achieve analytic relationships between different movement states, which is useful for rapid computing of the COMs trajectory [4]. It also solves the problem of the singularity for position controlling by bending knees [5]. In [6], the linear inverted pendulum model was simplified into the Running$-$Cart$-$Table model, which was utilized to enhance the stability of the HRP robot by introducing the pre$-$view trajectory of the ZMP. In [7], based on LIPM, the whole body dynamic model was refined containing the mass of the upper body, the swing leg and the supporting leg, which was a developed description of the bipedal walking motion.

However, the linear inverted pendulum model requires to keep the height of COM constant and the knee joint needs to be applied with high torque, due to bending for virtual constraint. It is negative for energy efficiency of bipedal walking [8]. Stretching knee under the help of toe and heal rotation has been developed for robots based on LIPM to improve the energy efficiency [9] [10] [11]. In the methods, the height of COM was kept constant while the rotations of toe and heal providing compensation height for the stretched supporting leg.

On the other hand, IPM without actuation normally characterizes the robots with stiff legs and can walk passively under gravity [2] [12] [13]. The shorter moment arm of driving joint in IPM is an advantage over LIPM to save energy, because the torque required decreases. IPM without bending knees for actuated robots was also applied in sagittal plane [14] and in three-dimensional space [5] [15]. However, the models proposed in [5] [15] had limits for humanoids' gait planning based on ZMP criterion, as the moment around ZMP about either x or y axis needs to be zero while their models considered in polar coordinate didn't guarantee zero moment around pivot p : (x_p, y_p) in sagittal and lateral planes. We derived the dynamic equation analytically of spherical IPM satisfying zero moment around supporting pivot p on the ground in forward and lateral directions and demonstrated the high coupling of it. Therefore, another model with the advantage of lower computing cost while with high energy efficiency for bipedal motion planning needs to be introduced.

In this paper, cylindrical-inverted pendulum (CIPM) which is based on the improvement of the conventional IPM, is a compromise between LIPM which has the advantage of computing and IPM which indicates high energy efficiency. The relationships with low coupling between the dynamic equation variables are easier for computing than IPM. Besides, CIPM has the advantage of lower energy consumption than LIPM, which can be validated by mathematic analysis and simulations.

In the second chapter of the paper, we introduced a bipedal robot and its model for simulation and the 3$-$dimensional CIPM. Firstly, the dynamic equation of IPM is derived and found unfeasible for motion planning. Secondly, the differential equations of CIPM are obtained, illustrating the low coupling as well as computing advantage. Finally, CIPM's advantage of energy efficiency over LIPM is discussed by mathematic analysis. In the third chapter, method of walking pattern generation based on CIPM is introduced, using conventional ZMP chasing method. In the fourth chapter, to demonstrate proposed method, the simulation model with dynamical characters measured in base of real small sized humanoid robot in BIT was used under different walking speeds based on CIPM. The consequences show the CIPM

The corresponding author is Runming Zhang (3120185113@bit.edu.cn).
This work was supported by the National Natural Science Foundation of China under Grants 61673069, 91748202, 61320106012.
[1]Intelligent Robotics Institute, School of Mechatronical Engineering, Beijing Institute of Technology, 5 Nandajie, Zhongguancun, Haidian, Beijing, 100081, China
[2]Beijing Advanced Innovation Center for Intelligent Robots and Systems, Beijing Institude of Technology, China
[3]Department of Mechanical Engineering and Intelligent Systems, The University of Electro-Communications, Tokyo, Japan

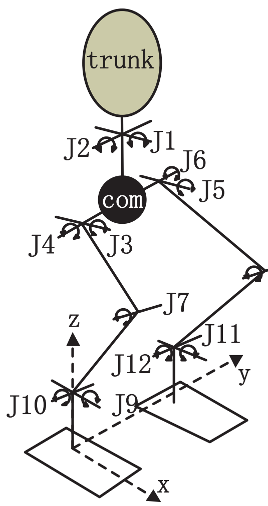

Fig. 1. Model of small sized humanoid robot and diagram of robot's joints distribution.

TABLE I
PARAMETERS OF THE MODEL OF BIPEDAL ROBOT

Parameter	Value
Length of thigh	0.12 m
Length of shank	0.12 m
Mass of lower limb	1.1 kg
Mass of trunk and waist	1.2 kg
Width of hip	0.06 m

can be implemented for different walking speeds and the energy consumption is less than that of LIPM for the same walking performance.

II. MODEL INTRODUCTION AND COMPARISON AMONG LIPM, IPM AND CIPM

As is shown in Fig.1, the tested humanoid robot totally has 12 degree of freedoms (DOF). Joint 1 along forward direction provides the DOF for torso to pitch, while joint 2 making the torso roll around the x axis of task coordinate. The motions of waist joints are for maintaining the posture of trunk, while lower limb joints adjusting the center of mass (COM) to keep ZMP in the supporting polygon. Joints 3, 5 and joints 4, 6 at hips provide the rotations in sagittal and lateral plane of thigh to complete the walking motion. The joints 7, 8 on the knees, provide one DOF for shanks' swaying to change the length of leg. Joints 10, 12 allow ankles pitch about the shanks while joints 9, 11 making the feet roll about ankles. Ankle joints are critical for posture controlling and stabilizing, as the paw of supporting foot must be parallel to the ground while adjusting the ZMP. Because lacking of the DOF for the vertical rotation for two thighs in the waist of robot, the motion of yaw can only be considered on the subsequent type in our future work. The task coordinate of robot lies at the middle of two paws. And the parameters of the tested model are listed at TableI. Three models, IPM, LIPM and CIPM to be compared with are descriptions of mass point's movement

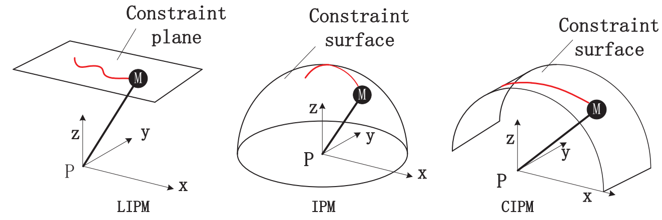

Fig. 2. Overview of three bipedal walking dynamic models.

in space under gravity with corresponding constraints. The common feature is that the moment around supporting pivot P on the ground which is commonly defined as ZMP is zero. To complete forward locomotion, virtual constraints were implemented for planning travelling trajectories of bipedal robots. Three-dimensional inverted pendulum model (IPM) restricts the length of stance leg and LIPM restricts the height of COM during walking while CIPM restricts the radius of displacement of COM in sagittal plane.

A. Features of IPM and dynamic equation derivation

IPM used to be common in passive walking experiments, where gravity is the only energy input for forward locomotion. However, this kind of passive walking occurs in sagittal plane and is hard to extend to 3 dimensional space. So, in IPM mode of 3 dimensional bipedal walking, the COM travels on spherical surface whose radius is the length of supporting leg as is shown in Fig.2. The spacial constraint of movement variables for IPM is shown in (1) (2). In (2), A represents a polynomial containing trigonometric functions of φ, ψ which are pitch and roll angles for the COM as shown in Fig.3. $A = \tan^2\psi + \tan^2\varphi + 1$

$$(x - x_p)^2 + (y - y_p)^2 + z^2 = r^2 \tag{1}$$

According to the spherical surface constraint, the Cartesian coordinate variables for IPM are expressed as

$$x - x_p = r \tan\varphi A^{-\frac{1}{2}}, y - y_p = r \tan\psi A^{-\frac{1}{2}}, z = rA^{-\frac{1}{2}} \tag{2}$$

We implemented Euler-Lagrange function to obtain the relationship between passive angles and the acceleration of COM.

$$L = T - P = m\sqrt{(\dot{x})^2 + (\dot{y})^2 + (\dot{z})^2}/2 - mgz \tag{3}$$

$$\begin{aligned} moment_{y_p}^{x} &= \frac{\partial}{\partial t}\frac{\partial L}{\partial \dot{\varphi}} - \frac{\partial L}{\partial \varphi} = 0 \\ moment_{x_p}^{y} &= \frac{\partial}{\partial t}\frac{\partial L}{\partial \dot{\psi}} - \frac{\partial L}{\partial \psi} = 0 \end{aligned} \tag{4}$$

$$\begin{aligned} \begin{bmatrix} A^{\frac{1}{2}} \\ A \\ A^2 \end{bmatrix}^T \begin{bmatrix} g\tan\psi \\ (1+\tan^2\psi) r\ddot{\psi} + 2\dot{\psi}^2 r\tan\psi \\ 2\dot{\psi}^2 r\tan\psi - 2\dot{\psi}\dot{\varphi} r\tan\varphi \end{bmatrix} = 0 \\ \begin{bmatrix} A^{\frac{1}{2}} \\ A \\ A^2 \end{bmatrix}^T \begin{bmatrix} g\tan\varphi \\ (1+\tan^2\varphi) r\ddot{\varphi} + 2\dot{\varphi}^2 r\tan\varphi \\ 2\dot{\varphi}^2 r\tan\varphi - 2\dot{\varphi}\dot{\psi} r\tan\psi \end{bmatrix} = 0 \end{aligned} \tag{5}$$

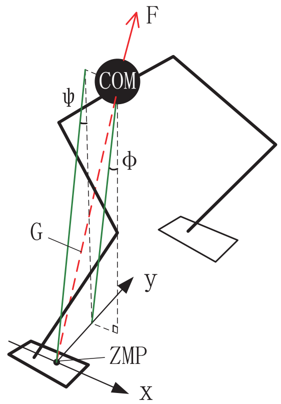

Fig. 3. Relationship between structures and pitch and roll angles. Green lines are projections to sagittal and lateral planes.

To keep the moment around supporting pivot zero in x and y directions, the dynamic equations of IPM should be as (5). The expressions has been largely simplified by assuming three and more orders of tangent function be zero. However the relationship between angular accelerations and current states is still complex and strongly coupled. This causes heavy load for online computing of desired ZMP trajectories and motion planning.

B. Force analysis for LIPM

LIPM proposed by Kajita, requires COM traveling on a horizontal plane with restricted height and reduce the load of computing. The joints of lower limbs cooperate to maintain the virtual constraint, making the locomotion follow desired trajectory. The relationship between Cartesian coordinate variables in LIPM are linear differential equations with one element, which can be expressed as (6) [6].

$$\begin{array}{c} \ddot{x} - {w_{lipm}}^2 (x - x_p) = 0 \\ \ddot{y} - {w_{lipm}}^2 (y - y_p) = 0 \\ w_{lipm} = \sqrt{\frac{g}{h}} \end{array} \tag{6}$$

And the characters such as step period T, step length S can be derived from pre-defined width of the hip W and the height of COM h. Parameters for bipedal walking can be designed owe to linear differential equations and analytic functions of x, y, making trajectory planning simple. The only difference between x and y is that y returns to $y|_{t=0}$, while x moves forward to $S/2+x_p$. The resultant force from p to COM and the torques applied on joints for locomotion of LIPM can be expressed as (7) (8). And the torques applied on joints for locomotion and maintaining constraints can be derived from Euler-Lagrange function.

$$F_{lipm} = m\ddot{y}\,\frac{\sqrt{(x - x_p)^2 + h^2 + (y - y_p)^2}}{y - y_p} \tag{7}$$

$$\tau = {J_{l,\theta_i}}^T F_{lipm} \tag{8}$$

$$\int_0^T P^e dt = \int_0^T UIdt = K_{I \to \tau_\theta} U \int_0^T \tau dt \tag{9}$$

$$W_{lipm} = \int_0^T |F_{lipm} \frac{\partial L_{lipm}}{\partial t}| dt \tag{10}$$

$L_{lipm}(t)$ is an unlinear function consist of exponential function of time, representing the distance from pivot to COM in 3 dimensional space for LIPM. J is the Jacobian matrix of endpoint's displacements to joints' generalized coordinates. In (9) and (10), $P^e = UI$ represents the total power consumption of the dissipative robot system, and W represents the mechanical work for driving.

C. CIPM and its advantages of computing and energy efficiency

The CIPM introduced in this paper has constant distance from COM to pivot p in sagittal plane and there is no constraint in lateral plane, and the definition is shown in (11). The purpose of introducing CIPM is to set up virtual movement constraint to import the advantage of computing with low coupling. Furthermore, CIPM doesn't need much bending of the supporting knee as the height of COM is not constant and in the middle of single supporting phase (SSP) the height of COM reaches the maximum. At the entry of SSP, the COM has obtained kinetic energy from double supporting phase (DSP) and ready to convert it to potential energy. We indicated the initial velocity of SSP, the velocity for launching, with expression V_{lau} and desired cylindrical surface should always be tangent to V_{lau}. In CIPM, the axis of the cylindrical surface is required to cross ZMP and be vertical to sagittal plane. Movement variables of CIPM have the relations as shown in (12) (13) where r is the constant radius of the cylinder.

We choose different kinds of coordinate system to describe the COM locomotion in three models. In IPM, according to the spherical surface constraint, the relationships between pitch, roll angles and their differentials are easier to be expressed than Cartesian coordinate variables. Thus, for CIPM, pitch angle φ and extension length in y direction can better describe the movement on a cylindrical surface.

$$(x - x_p)^2 + z^2 = r^2 \tag{11}$$

$$\ddot{\varphi}\, r - g \sin\varphi = 0 \tag{12}$$

$$(g - \ddot{\varphi}\, r \sin\varphi - (\dot{\varphi})^2 r \cos\varphi)(y - y_p) = \ddot{y}\, r \cos\varphi \tag{13}$$

In this equation, $\sin\varphi = (x - x_p)/r$ and the moment around the axis of cylinder must be zero. Similar to that in LIPM, the initial position of COM in x has the distance of $-S/2$ to x_p and the COM returns back in y direction at the end of SSP. If first order derivative of φ is multiplied to the left and right sides of the first equation in (12), and integrate time, it can be expressed as

$$\begin{array}{c} \frac{r\dot{\varphi}^2}{2} = -g\cos\varphi + C \\ (3gcos\varphi - 2C)(y - y_p) = \ddot{y}\;\; r \end{array}$$

Although there is no analytical dynamic equations for COM's trajectory, the relationships between states are clearer than in IPM. If a particularly small step length is required, the sinusoidal function of pitch angle of humanoid's COM

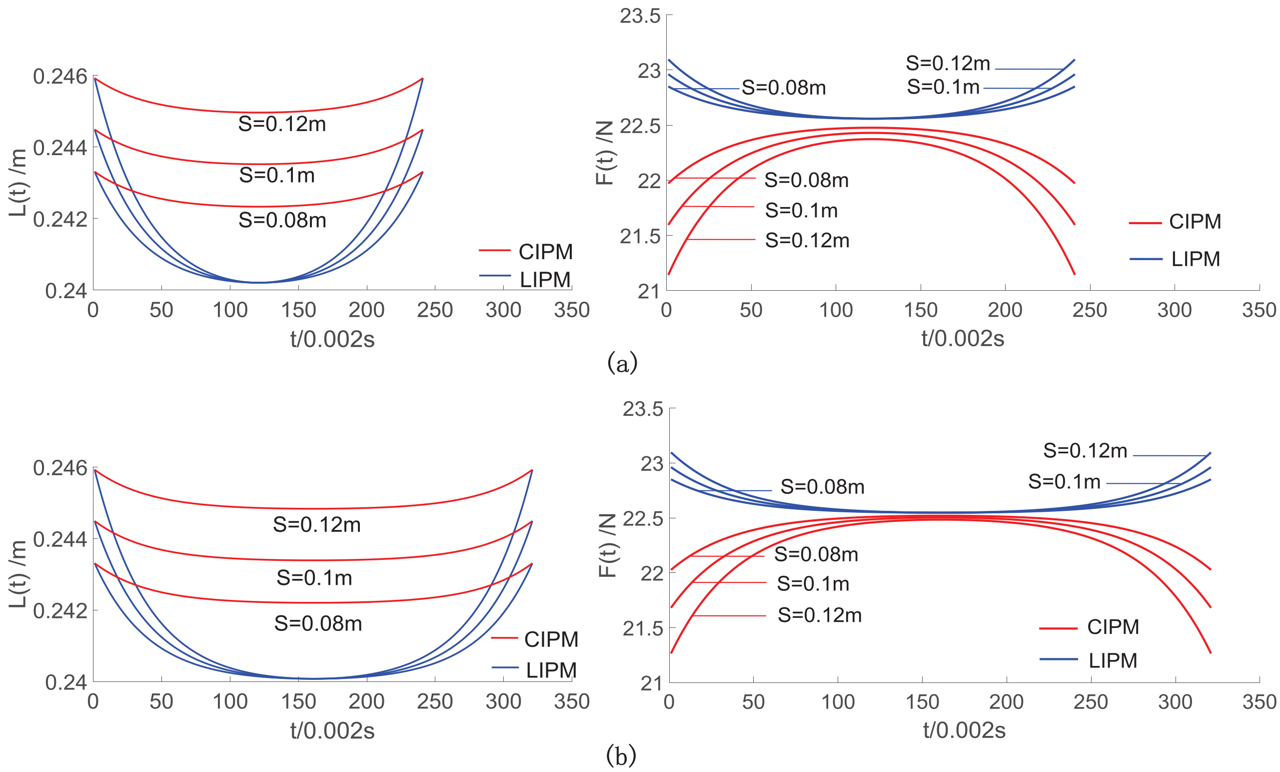

Fig. 4. L(t) and F(t) comparisons between LIPM and CIPM for three step lengths with two step periods. In (a), the period is 0.6s and in (b) the period is 0.8s.

$\sin\varphi$ can be approximated as φ. Linearized expression of the differential equations of CIPM are shown in (14) (15).

$$\ddot{\varphi}\, r = g\varphi \tag{14}$$

$$(3g - 2C)(y - y_p) = r\,\ddot{y} \tag{15}$$

$$\varphi = C_{11}e^{w^{\varphi}_{cipm}t} + C_{12}e^{-w^{\varphi}_{cipm}t} \tag{16}$$

$$y - y_p = C_{21}e^{w^{y}_{cipm}t} + C_{22}e^{-w^{y}_{cipm}t} \tag{17}$$

In CIPM, the variable of pitch angle has similar differential equation to variable x's in LIPM. The constants C, C_{11}, C_{12}, C_{21}, C_{22} are obtained by boundary conditions and predefined parameters.

Generally, the step length cannot be regulated too small for walking task. The dynamic in sagittal plane of CIPM is an one dimensional nonlinear system, with lower coupling comparing to IPM. Trajectory of pitch angle φ can be derived from the initial and terminal conditions with the method of Runge Kutta. The trajectory of COM in y direction can be obtained consequently with the same method. As the mass is concentrated at one point COM, the pendulum model is an equivalent to a multi-link mechanism with COM located on its endpoint. Resultant force from the supporting pivot to push the COM in CIPM is expressed as (18). Then the mechanical works of driving COM can be obtained according to (18) (19).

$$F_{cipm} = \frac{m(3gcos\varphi - 2C)L_{cipm}(t)}{r} \tag{18}$$

In this equation, $L_{cipm}(t)$ containing exponential expressions of time represents the distance from pivot to COM in 3 dimensional space for CIPM.

$$W_{cipm} = \int_0^T |F_{cipm}\frac{\partial L_{cipm}}{\partial t}|dt \tag{19}$$

Three step lengths S with two step periods T were selected for comparing the mechanical works for two models. In time domain, $L(t)$ and $F(t)$ have different trends for two models. The six forward speeds with 2 Ts and 3 Ss were tested analytically and the comparison of resultant force and length of pivot-to-COM for two models is shown in Fig.4. As the Fig.4 indicates, during SSP the forces of CIPM and variation of $L(t)$ are both less than those of LIPM. Thus, for an ideal particle model, it can be demonstrated that the demand of mechanical power is less in CIPM than in LIPM. However, the evaluation of energy efficiency is based on the sum of energy consumption composed of thermal dissipation, impact loss and mechanical work, for an electrically driven humanoid robot. To demonstrate the average energy cost is less in CIPM than in LIPM for walking task, simulations need to be applied and that will be introduced in the chapter 4.

III. Bipedal Walking Planning Based on CIPM

The walking pattern is divided into three parts for one step: 2 double supporting phases (DSP) and a single supporting

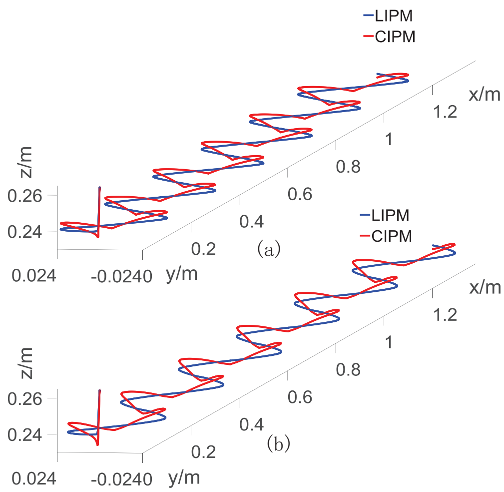

Fig. 5. Trajectories of COM in world coordinate frame computed for tested speeds. It is illustrated that faster walking for CIPM and LIPM requires larger margin of COM displacements in vertical direction and less displacements in lateral direction. (a) represents the planned trajectories for CIPM and LIPM for 0.125m/s's walking. (b) represents the walking with speed of 0.2m/s.

phase (SSP). At the start of the first DSP, the current height of COM of the robot is minimum for whole step, with velocity zero. The velocity of the COM needs to be the largest during step at the SSP entry, for converting kinetic energy into potential energy. Then, to achieve the forward motion, energy is injected by two supporting legs pushing the COM of robot to the initial position of SSP. In this paper, the two legs in DSP were equalized to 5-link closed loop mechanism which moves the COM to the next SSP. Thus, the characters of CIPM and LIPM etc. are only discussed in SSP, when the moment of the robot around ZMP beneath the supporting foot be zero and the motion of COM has the feature of specific space constraints.

$$P_y = \frac{\sum\limits_i m_i(\ddot{z}_i + g)y_i - \sum\limits_i m_i \ddot{y}_i z_i}{\sum\limits_i m_i(\ddot{z}_i + g)} \tag{20}$$

$$P_x = \frac{\sum\limits_i m_i(\ddot{z}_i + g)x_i - \sum\limits_i m_i \ddot{x}_i z_i}{\sum\limits_i m_i(\ddot{z}_i + g)} \tag{21}$$

To compare the energy cost between CIPM and LIPM, two desired speeds were tested by simulation in this paper. The step lengths were selected as 0.1m and 0.12m for a model of small sized robot. Periods of step were selected as 0.8s and 0.6s which were tested in previous bipedal investigations [16] [17] and the duration of DSP was set as 20 percent of the walking period [18]. Reference ZMP was planned according to the structural parameters, required walking speeds and step lengths. To meet the stability principle of ZMP, the displacement of COM should satisfy the equation (20) and (21) in DSP. The trajectories of the COM and footholds based on CIPM and LIPM are derived consequently from ZMP references and (12) (13) (20) (21) and the diagrams of COM trajectory are shown in Fig.5.

IV. Demonstration by simulation

As the analysis in chapter 2 is based on simple model of mass point with two links and one driving joint, the dynamic model for simulation should be strictly corresponding to real robot to get detailed pattern of the torques for joints in CIPM and LIPM's walking. First, we set up requirements of step lengths and periods, refer to previous investigations about human beings and robot's bipedal walking's, with the consideration of the little size of tested model. After computing the dynamics of designated model, the reference of trajectories of COM and the footholds were obtained. Then the desired joints angles were generated by inverse kinematics.

In the simulation computing step length was 2ms and the torque applied on joints in walking gaits were acquired by dynamic processor in V-REP as is shown in Fig.6. The simulation consists of twenty steps for different walking speeds with the motion of setting off at the start of the walking and the diagram only intercept a few steps for discussing. In Fig.6, the torque of hip's rolling during walking is less than those applied on knee joints and the difference of it between CIPM and LIPM is little. However, the amplitude of pitching torque on hip joints for two models are less than rolling torques and faster walking causes larger magnitude of vibration. As for pitching torque on hip joint, there is no obvious advantage of CIPM over LIPM, since the hip pitching torque for LIPM is larger than that for CIPM for most of the time in SSP. The torque exerted by knee joint for LIPM in SSP is larger than that for CIPM, with different walking speeds, coinciding with mathematic analysis in chapter 2. Note that the knee torque in DSP for CIPM is sometimes larger than that for LIPM as shown in Fig.6, because of the increasing of COM height in DSP at the start of one step for CIPM which is undesired for LIPM.

In bipedal walking, energy is used for locomotion with desired speed, maintaining potential energy and complementing the loss caused by environment interactions. Thus, different from machines whose mechanical cost can be expressed as $P = FV$, energy input of bipedal locomotion is dissipated throughout the time [19]. Different with pure mechanical works, the total energy consumption should be expressed as $\int UIdt = \int UK\tau dt$, in which I is assumed related to torque applied on actuators. Because the speed of walking is regulated, the denominator of cost of transport (COT) is eliminated in the comparison between LIPM and CIPM. In this paper, time integration of torques equals COT multiplied by speed S/T. And the advantage of CIPM of energy efficiency for bipedal walking can be shown with different speed requirements, as the duration of DSP, during which torque applied on knee joint can be little larger for CIPM is much shorter than SSP.

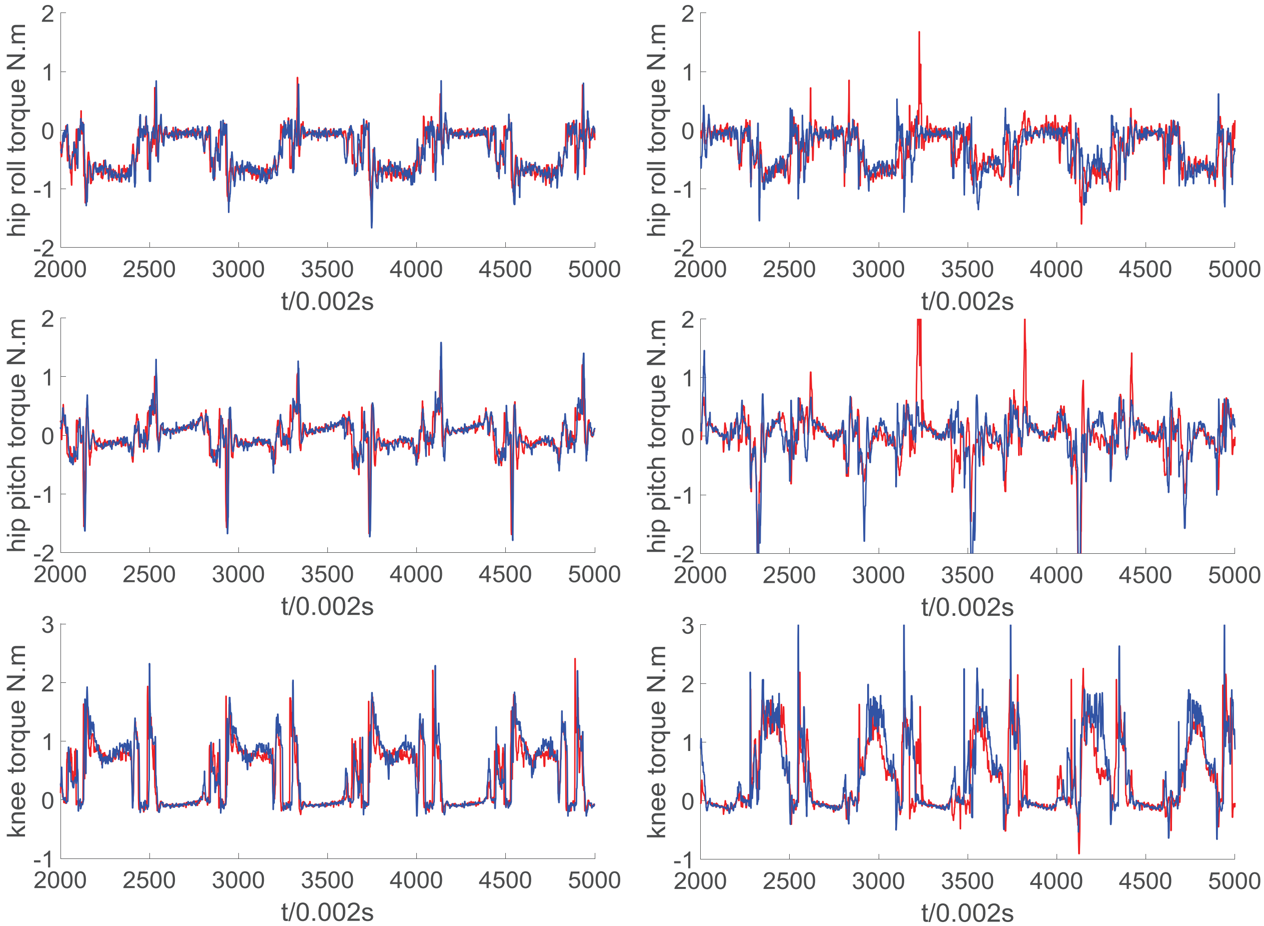

Fig. 6. The left part indicates the torque applied on lower limb joints with walking speed 0.125m/s and on the right 0.2m/s. The red lines represents the torque applied on CIPM walking and blue ones refers to LIPM. The first row of figure represents the torques applied on hip joint in x direction and the second represents the torque applied on hip joint in y direction. The third row indicates the torque exerted by knee actuator during the walking gait.

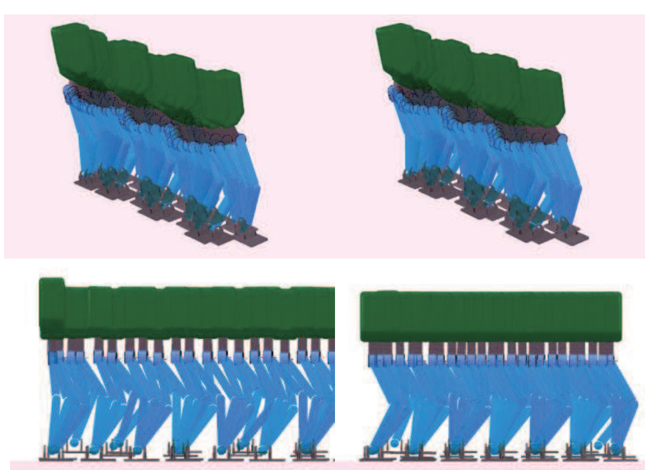

Fig. 7. Interception of walking simulation of 0.125m/s. On the left is the CIPM walking, while on the right LIPM. Two models have similar magnitude of lateral displacements while walking.

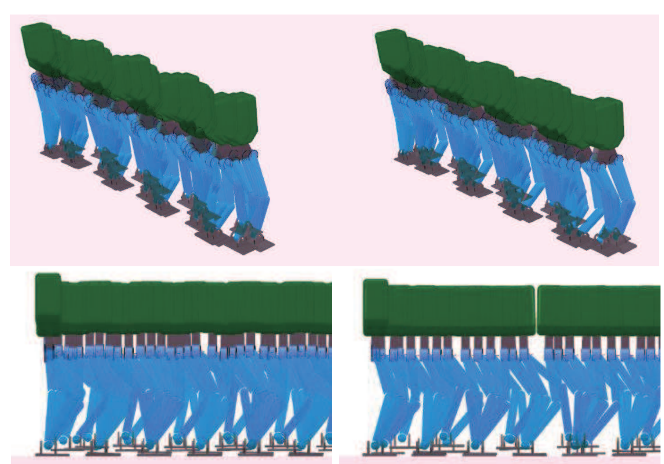

Fig. 8. Interception of walking simulation of 0.2m/s. On the left is the CIPM walking, while on the right LIPM. The difference of vertical movement between two models rises for a larger speed, as the radius of the cylinder in CIPM as well as the step length increase.

V. Conclusions

This paper proposed a new method CIPM for three dimensional bipedal walking planning, which combines the advantage of lower energy consumption as IPM and lower computing cost as LIPM. Computing advantage over IPM and less desired work than LIPM in SSP are demonstrated by dynamic analysis, and the total energy consumption of CIPM less than that of LIPM is validated by simulation. The consequences indicate that the CIPM is a feasible method for controlling bipedal walking for different speeds and has the advantage of high energy efficiency over LIPM.

The disadvantage of this paper is that the time integration of current is simply equivalent to that of torque ignoring the friction loss in transmission and electromagnetic characters inside the actuators. A more precise model for energy consumption evaluation will be developed in the future. What's more, when the dynamic equations in sagittal and lateral planes should be simplified and linearized lacks analysis under the condition that φ is small. So in the future, we need to develop correlated method for controlling bipedal walking with large range of parameters in base of CIPM.

References

[1] H. Hemami and C. L. Golliday, "The inverted pendulum and biped stability," *Mathematical Biosciences*, vol. 34, no. 1, pp. 95–110, 1977.

[2] T. McGeer, "Passive dynamic walking," *The International Journal of Robotics Research*, vol. 9, no. 2, pp. 1–10, 1990.

[3] S. Kajita and K.Tani, "Study of dynamic biped locomotion on rugged terrain derivation and application of the linear inverted pendulum mode," in *IEEE International Conference on Robotics and Automation*, vol. 2, 1991, pp. 1405–1411.

[4] S. Faraji and A. J. Ijspeert, "3LP: A linear 3D-walking model including torso and swing dynamics," *The International Journal of Robotics Research*, vol. 36, no. 4, pp. 436–455, 2016.

[5] A. Sekiguchi, Y. Atobe, K. Kameta, Y. Tsumaki, and D. N. Nenchev, "A walking pattern generator around singularity," in *IEEE-RAS International Conference on Humanoid Robots*, 2006, pp. 270–275.

[6] S. Kajita, F. Kanehiro, K. Kaneko, K. Fujiwara, K. Harada, K. Yokoi, and H. Hirukawa, "Biped walking pattern generation by using preview control of zero-moment point," in *IEEE International Conference on Robotics and Automation*, vol. 2, 2003, pp. 1620–1626.

[7] T. Sato, S. Sakaino, and K. Ohnishi, "Real-time walking trajectory generation method with three-mass models at constant body height for three-dimensional biped robots," *IEEE Transactions on Industrial Electronics*, vol. 58, no. 2, pp. 376–383, 2011.

[8] B. V. Bram Vanderborght and R. V. Ham, "Objective locomotion parameters based inverted pendulum trajectory generator," *Robotics and Autonomous Systems*, vol. 56, no. 9, pp. 738–750, 2008.

[9] T. K. J. Englsberger, S. Bertrand, J. Pratt, C. Ott, and A. Albu-Schäffer, "Trajectory generation for continuous leg forces during double support and heel-to-toe shift based on divergent component of motion," *IEEE/RSJ International Conference on Intelligent Robots and Systems*, pp. 4022–4029, 2014.

[10] G. W. Robert J. Griffin, S. Bertrand, A. Leonessa, and J. Pratt, "Straight-leg walking through underconstrained whole-body control," *IEEE/RSJ International Conference on Intelligent Robots and Systems*, 2017.

[11] M. B. Shuuji Kajita and R. Cisneros, "Biped walking pattern generation based on spatially quantized dynamics," *IEEE-RAS International Conference on Humanoid Robots*, pp. 599–605, 2017.

[12] T. Geng, "Online regulation of the walking speed of a planar limit cycle walker via model predictive control," *IEEE Transactions on Industrial Electronics*, vol. 61, no. 5, 2014.

[13] N. C. Rafael Stanley, J. Manuel, and I. Zannatha, "Efficient mechanical design and limit cycle stability for a humanoid robot: An application of genetic algorithms," *Neurocomputing*, pp. 72–80, 2017.

[14] J. Y. K. Ill Woo Park and J. H. Oh, "Online biped walking pattern generation for humanoid robot khr-3(kaist humanoid robot - 3: Hubo)," *Multibody System Dynamics*, no. 3, pp. 398–403, 2006.

[15] T. A. Taisuke Kobayashi and Y. Hasegawa, "Adaptive speed controller using swing leg motion for 3-d limit-cycle-based bipedal gait," *Nonlinear Dynamics*, vol. 84, no. 4, pp. 2285–2304, 2016.

[16] S. K. Mitsuharu Morisawa, K. Kaneko, K. Harada, F. Kanehiro, K. Fujiwara, and H. Hirukawa, "Pattern generation of biped walking constrained on parametric surface," *IEEE International Conference on Robotics and Automation*, pp. 2405–2410, 2005.

[17] K. H. Takashi Takuma, "Controlling thewalking period of a pneumatic musclewalker," *The International Journal of Robotics Research*, vol. 25, no. 9, pp. 861–866, 2005.

[18] C. O. Johannes Englsberger and A. Albu-Schäffer, "Three-dimensional bipedal walking control based on divergent component of motion," *IEEE Transactions on Robotics*, vol. 31, no. 2, pp. 355–368, 2015.

[19] A. W. Sangok Seok, M. Y. M. Chuah, D. J. Hyun, J. Lee, D. M. Otten, J. H. Lang, and S. Kim, "Design principles for energy-efficient legged locomotion and implementation on the mit cheetah robot," *IEEE/ASME Transactions on Mechatronics*, vol. 20, no. 3, pp. 1117–1129, 2015.